EUROPEAN ORGANIZATION FOR NUCLEAR RESEARCH

CERN–PPE/94–87
8 June 1994

NEUTRINO OSCILLATION EXPERIMENTS AT ACCELERATORS

L. Camilleri
CERN, Geneva, Switzerland

Talk given at the 6th International Workshop on Neutrino Telescopes
Venice, Italy, 22–24 February 1994

1 Introduction

If neutrinos have a non-zero mass it is possible that they will mix such that a given flavour neutrino could oscillate into another [1]. In the case of two-neutrino mixing such as ν_μ and ν_τ, the probability for finding a ν_τ having started with a ν_μ is given by

$$P_{\mu\to\tau} = \sin^2 2\theta \sin^2 2\pi L / \lambda$$

where θ = mixing angle
L(km) = distance between source and detector
λ = oscillation length
$= 5\ E_\nu\ (\mathrm{GeV})/\Delta m^2\ (\mathrm{eV}^2)$
with E_ν = neutrino energy
$\Delta m^2 = m^2_{\nu_\tau} - m^2_{\nu_\mu}$

In general the detector must be installed far enough away from the source to give the original flavour time to oscillate into the new state. Two regimes are of importance:

- Small Δm^2. Then, for the probability of oscillation to be significantly different from zero the smallness of Δm^2 must be compensated either by a large L or a small E_ν.
- Small λ (small E_ν or large Δm^2). If λ is much smaller than the detector size, then several oscillations can occur within the detector. In this case $\sin^2 (2\pi L / \lambda)$ averages to 1/2, yielding

$$P_{\mu\to\tau} = \frac{1}{2}\sin^2 2\theta$$

The present state of the exclusion plot for $\nu_\mu \to \nu_\tau$ is shown in Fig. 1. The limit set [2] by E531 at Fermilab is $\sin^2 2\theta < 5\times10^{-3}$ at large Δm^2. Improving this limit is important as it would probe a range of Δm^2 and $\sin^2 2\theta$ in which oscillations are expected [3] if,

- the lower than expected solar neutrino [4] rates are due to the MSW effect [5], (oscillations in matter) and the neutrino masses follow the same hierarchy as the quark masses:
$$m_{\nu_e} : m_{\nu_\mu} : m_{\nu_\tau} \sim m_u^2 : m_c^2 : m_t^2$$
as given by a GUT see-saw mechanism [6, 7];
- the dark matter conjectured to explain the rotational velocity curve of galaxies [8] is composed of tau neutrinos.

Also shown in Fig. 1 is the region of oscillation parameters favoured by Kamiokande [9] if its observations of a lower ν_μ/ν_e ratio than expected in atmospheric neutrinos is due to oscillations. Probing this region of the exclusion plot with an accelerator experiment requires low energy neutrinos and a large detector-source distance.

2 The Experiments

There are currently one neutrino oscillation running at an accelerator (LSND [10] at Los Alamos), two installing at CERN (CHORUS [11] and NOMAD [12]), one approved [13] at Brookhaven (E889) and one approved [14] at Fermilab (E803). The type and energy of the beams used by these experiments, their detector-source distances, the mode of detecting oscillations and their status are listed in Table 1.

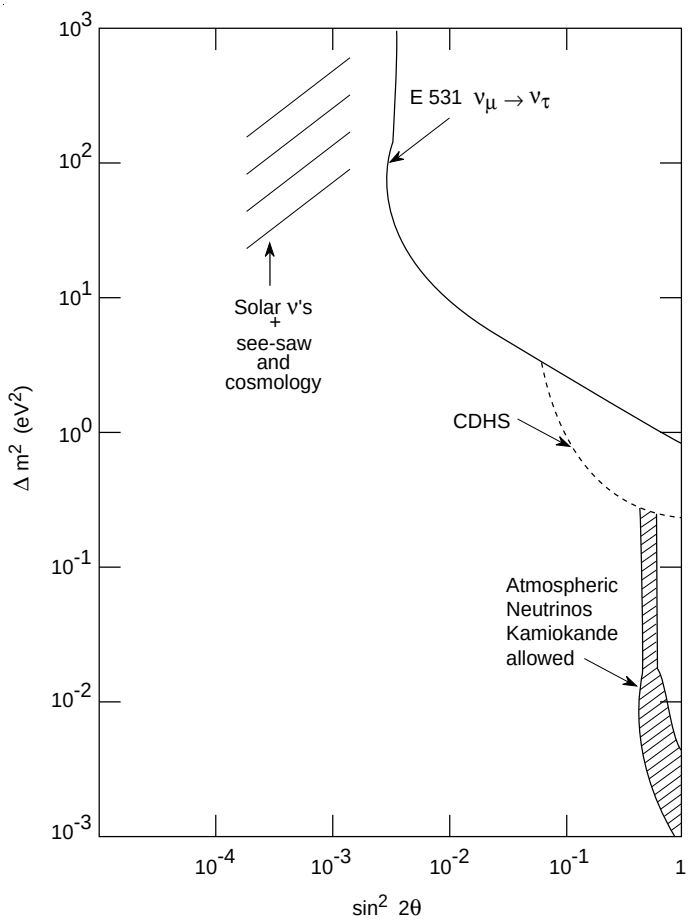

Figure 1: The present limit on $\nu_\mu \rightarrow \nu_\tau$ oscillations and the region allowed by the atmospheric neutrino results.

Table 1
Characteristics of Neutrino Oscillation Experiments at Accelerators

Experiments	Accel.	Beam	Typical energy	Distance	Mode	Status Start-up
LSND	LAMPF (Los Alamos)	ν_μ $\bar{\nu}_\mu$	0.1 GeV	27 m	ν_e, $\bar{\nu}_e$ Appear	Running Aug. 1993
CHORUS	SPS (CERN)	ν_μ	30 GeV	800 m	ν_τ Appear	Approved Apr. 1994
NOMAD	SPS (CERN)	ν_μ	30 GeV	800 m	ν_τ Appear	Approved Apr. 1994 ↓ Apr. 1995
E889	AGS (Brookhaven)	ν_μ	1 GeV	1 km, 3 km, 24 km	ν_μ Disapp. ν_e Appear	Approved 1997–98
E803	MAIN INJ. (FERMILAB)	ν_μ	10 GeV	470 m	ν_τ Appear	Approved 1998

2.1 *The Liquid Scintillator Neutrino Detector*

This experiment [10] (Fig. 2) running at LAMPF at LOS ALAMOS, uses a beam of neutrinos and antineutrinos coming from pion and muon decays

$$\pi^+ \rightarrow \nu_\mu \, \mu^+$$
$$\mu^+ \text{(at rest)} \rightarrow \bar{\nu}_\mu \, \nu_e \, e^+$$

The pions are produced by the interaction of the 780 MeV proton beam with a water and copper beam stopper.

The experiment looks for the oscillation of ν_μ's and $\bar{\nu}_\mu$'s into ν_e's and $\bar{\nu}_e$'s respectively. The interaction of neutrinos and antineutrinos are observed in a detector consisting of 200 tons of liquid scintillator placed in a tank 9 m long, 6 m in diameter and viewed by 850 photomultipliers.

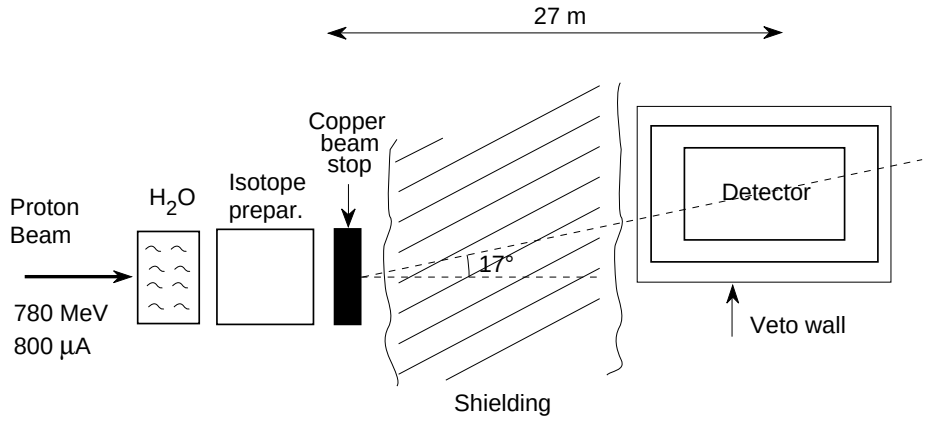

Figure 2: The Liquid Scintillator Neutrino Detector set-up.

The presence of ν_e and $\bar{\nu}_e$'s in the beam is detected via the reactions

$\nu_e + C \rightarrow e^- N$ yielding an electron in the energy range $60 \rightarrow 180$ MeV,

and $\bar{\nu}_e + p \rightarrow e^+ n$ yielding a positron in the energy range $37 \rightarrow 50$ MeV followed by 2.2 MeV gamma ray produced by the absorption of the recoil neutron on the free protons of the scintillator. This gamma ray is emitted within 0.5 ms and lm of the positron.

The electrons and positrons produced in these interactions emit scintillation and Cherenkov light which is recorded by the photomultipliers. The total number of photoelectrons produced by a contained particle is proportional to its path length in the detector and therefore to its energy. The energy resolution obtained is 3% at 100 MeV. It is important to have a good energy resolution as the experiment does not use a magnetic field and the electrons and positrons in the above reactions must therefore he distinguished from their different energy ranges. The location and timing of the hit photomultipliers yield a measurement of the position and direction of the observed particle with an accuracy of $\pm$ 9 cm and $\pm 10^o$ respectively at 100 MeV.

For maximal mixing, 33900 ν_e interactions yielding an electron with $60 < E_e < 180$ MeV are expected for an exposure of two years. In that time it is estimated that the background will amount to

2 events from cosmic rays.

9 events from ν_e's produced by decays in flight of muons and therefore energetic enough to produce electrons in the above energy range.

2 events from ν_e's produced by $\pi^+ \rightarrow \nu_e\, e^+$.

This overall background of 13 events allows a sensitivity of

$$\sin^2 2\theta > 2.7 \times 10^{-4} \quad \text{at} \quad 90\%\ \text{CL} \quad \text{for} \quad \Delta m^2 > 3\ \text{eV}^2.$$

In the case of $\bar{\nu}_\mu$'s, 33080 $\bar{\nu}_e$ interactions yielding a positron in the energy range $37 \rightarrow 50$ MeV are expected for an exposure of two years and if mixing is maximal. The background is estimated to be

2 events from cosmic rays.

8 events from π^-'s decaying in flight and producing μ^-'s which then decay at rest yielding $\bar{\nu}_e$'s in the correct energy range.

3 events from various less significant sources.

Again a total of 13 background events should allow the setting of a limit of

$$\sin^2 2\theta > 2.7 \times 10^{-4} \quad \text{at} \quad 90\%\ \text{CL} \quad \text{for} \quad \Delta m^2 > 1\ \text{eV}^2.$$

The region of the $\Delta m^2 - \sin^2 2\theta$ plot that LSND will be able to exclude, if no oscillations are found, is shown in Fig. 3 for $\nu_\mu \rightarrow \nu_e$ and $\bar{\nu}_\mu \rightarrow \bar{\nu}_e$ oscillations. Also shown are the limits that have been set by the Gosgen reactor disappearance experiment [15] ($\bar{\nu}_e \rightarrow \bar{\nu}_x$), the BNL E734 $\nu_\mu \rightarrow \nu_e$ experiment [16], the LAMPF E645 $\bar{\nu}_\mu \rightarrow \bar{\nu}_e$ experiment [17] and the LAMPF E764 $\nu_\mu \rightarrow \nu_e$ experiment [18].

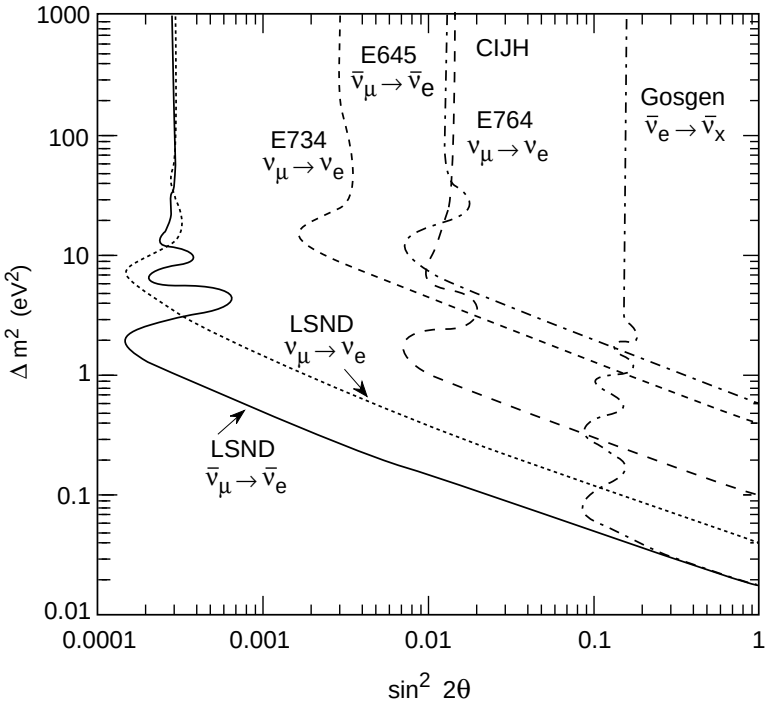

Figure 3: The region in $\Delta m^2 - \sin^2 2\theta$ that will be excluded by LSND together with present limits.

LSND took data in September and October 1993 and collected 2000 C of incident protons. The apparatus is performing as expected. The distributions of the number of hit phototubes/event shows the characteristic Michel electron spectrum. It is hoped to achieve the goal of 17 000 C in 1994 and 1995.

2.2 *The CERN Experiments*

The Neutrino Oscillation experiments at CERN are ν_τ appearance experiments in a beam consisting of ν_μ's. Any observation of ν_τ's, which are looked for through their charged current interaction $\nu_\tau N \rightarrow \tau^- X$, would indicate oscillations since the ν_τ content of the beam is negligible.

The 450 GeV proton beam extracted from the SPS impinges on a beryllium target. The resulting charged particles are made into an approximately parallel beam by a system of magnetic horns. This is then followed by a decay tunnel and an iron-earth absorber. The detectors are approximately 800 m away from the target.

The beam has been recently rebuilt and has been tested successfully in November 1993. It delivers neutrinos in two 6 ms long mini-spills separated by 2.6 s during each 14.4 s SPS cycle. The aim is to deliver 2×10^{13} protons on target (pot's) per SPS cycle for a total of 2.4×10^{19} pots over 2 years. The mean energy of the beam is 27 GeV. The contamination is 6% $\bar{\nu}_\mu$'s, 0.7% of ν_e's and 0.2% of $\bar{\nu}_e$'s.

During the November test run 1.7×10^{13} pots per SPS cycle have already been achieved. The beam is well centred at the detectors and has the expected profile and intensity as measured using the accompanying muons. Both experiments are satisfied with their background and trigger rates.

2.2.1 Neutrino oscillation magnetic detector

The principle used by NOMAD [12] (Fig. 4) in their search for $\nu_\tau N \rightarrow \tau^- X$ is to distinguish such events from background using purely kinematical cuts such as missing p_T, angular correlations etc. To do so very good energy, momentum and angular resolutions are needed. The τ is detected through its e $\bar{\nu}_e \nu_\tau$, μ $\bar{\nu}_\mu$ ν_τ, π^- ν_τ, ρ^- ν_τ, π^+ π^- π^- (n π^0) ν_τ decay modes. The target consists of the walls of the drift chambers used for momentum measurement. This introduces conflicting requirements as the drift chamber walls should be as heavy as possible in order to have many neutrino interactions and as light as possible in order to introduce little multiple scattering. The solution adopted by NOMAD is to use drift chambers made of a honey comb and kevlar skin structure. The target consists of 132 such planes spread over 4 m amounting to 3 tons in mass and to only 1 radiation length in total. The experiment re-uses the UA1 magnet inside which the drift chambers are placed. The momentum resolution, $\sigma(p)/p$, for an average length track is expected to vary between 3 and 5% over the momentum range relevant to the measurement.

The electromagnetic calorimeter needed to identify electrons and measure their energy and also to measure the energy of photons produced in the interactions, consists of lead glass and has an energy resolution of

$$\sigma\,(E)/E = 0.04/\sqrt{E} + 0.01$$

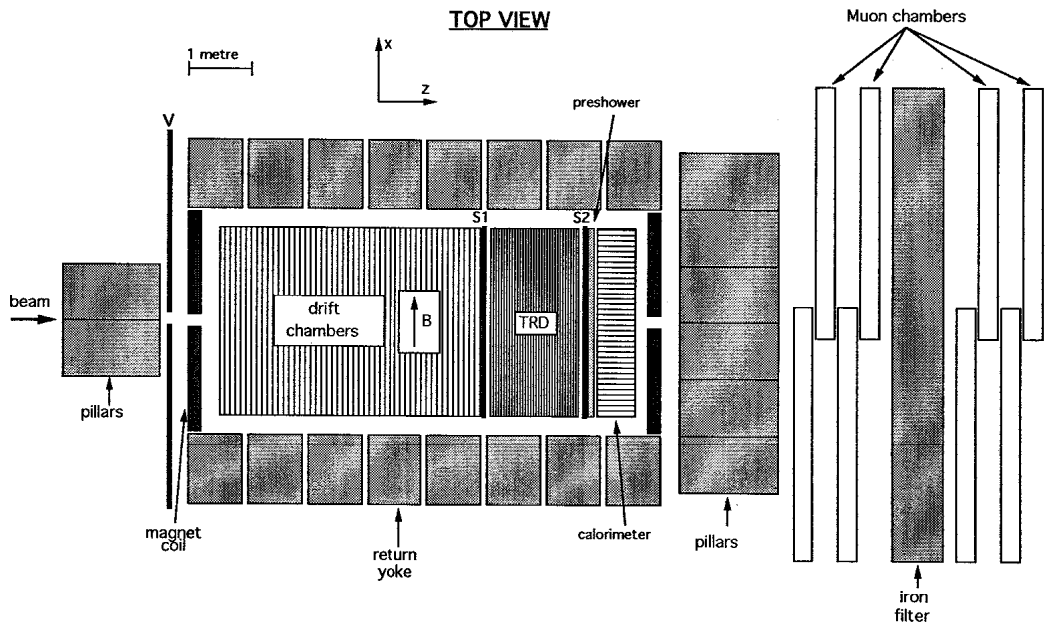

Figure 4: The NOMAD detector.

The detector also includes a plane of scintillation counters used to inhibit triggering on muons accompanying the neutrino beam and two planes of scintillation counters used for triggering. The discrimination between electrons and pions is provided by 9 transition radiation modules each consisting of 350 foils of polypropylene followed by a plane of straw tubes containing a Xenon-methane mixture to detect the transition radiation x-rays. A preshower consisting of a lead plane followed by a plane of horizontal tubes and a plane of vertical proportional tubes provides further e/π separation and a better position measurement for the photons that convert in the lead. Finally a system of muon chambers behind walls of iron provides muon identification. At a later date some of this iron will be instrumented to provide a hadron calorimeter.

As an example of the type of cuts used in the analysis the electronic decay of the τ will be considered.

$$\nu_\tau N \rightarrow X \tau^-$$
$$\hookrightarrow e^- \bar{\nu}_e \nu_\tau$$

The major background to this channel is caused by charged current interactions of the ~ 1% ν_e component of the beam

$$\nu_e N \rightarrow X e^-$$

In the plane perpendicular to the beam direction, angles between the electron and the resultant hadron vector, ϕ_{eh}, and between the missing p_T and the resultant hadron vector, ϕ_{mh}, are defined (Fig. 5a, b). For the background reaction, since the electron and the hadrons are the only particles in the reaction, ϕ_{eh} is sharply peaked at π (Fig. 5c). For the τ reaction, it is the τ that is back to back to the hadrons, and in the decay the electron will acquire some transverse momentum relative to the τ direction and will therefore not be necessarily back to back with the hadron (Fig. 5d). In the background reaction any missing p_T will arise either from missed neutrons and K_L^0 which contribute an enhancement in ϕ_{mh} around 0^0, or from mismeasurements which will give a flat contribution to ϕ_{mh} (Fig. 5e). In the τ reaction the missing p_T will be due to the two missing neutrinos and will therefore be centred on the τ direction, resulting in a peak in ϕ_{mh} at π (Fig. 5f).

It is clear that the ϕ_{eh} and ϕ_{mh} distributions are quite different for the background and signal. Similar distributions are used for the muonic and hadronic decay channels to reject the background.

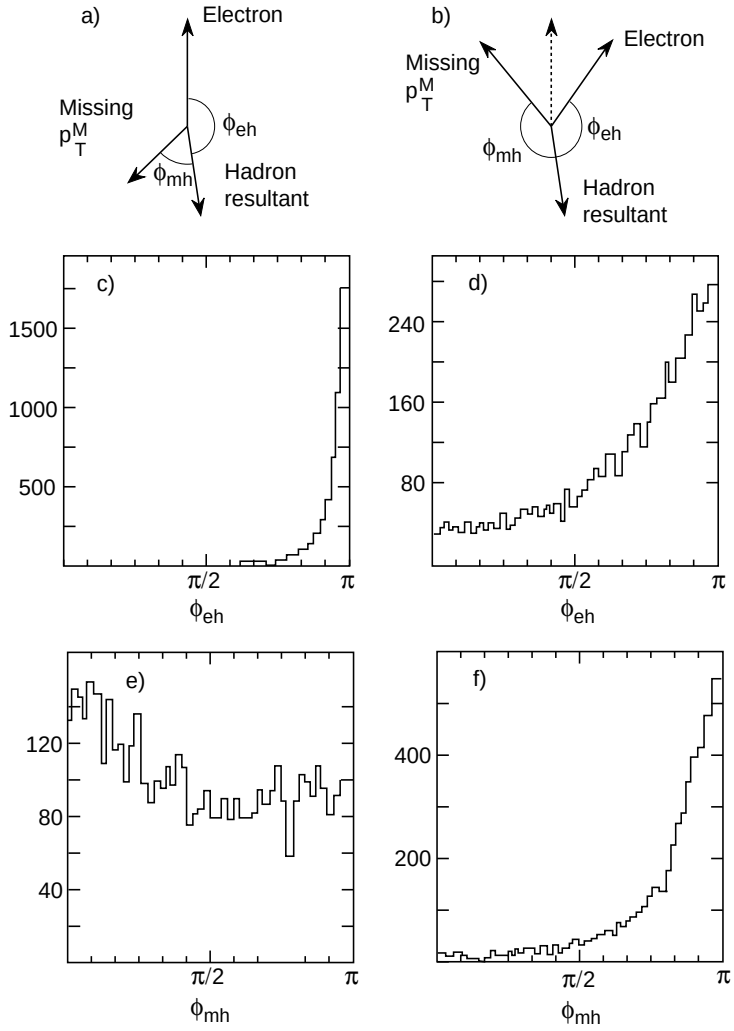

Figure 5: Example of kinematics cuts used by NOMAD to differentiate the background $\nu_e X \rightarrow e^- X$ from signal $\nu_\tau X \rightarrow \tau^- X$, $\tau^- \rightarrow e^- \bar{\nu}_e e \nu_\tau$
a), b) definition of the angles ϕ_{eh}, ϕ_{mh} for the background and the signal,
c), e) distribution of ϕ_{eh} and ϕ_{mh} for the background,
d), f) distribution of ϕ_{eh} and ϕ_{mh} for the signal.

2.2.2 CERN hybrid oscillation research apparatus

The principle used by CHORUS [11] (Fig. 6a) to recognise the presence of a τ meson is to observe the finite path of the τ meson before it decays. Thus a track with a kink would signal a τ decaying into a single charged particle whereas a track splitting into three others would signal a τ decaying into three charged particles. However, typical τ decay paths are < 1 mm at these energies. The target must therefore be active and have very good spatial resolution. This has led to the choice of emulsions as the target material. A total of 800 kg will be used amounting to 4 radiation lengths. A detail of the target area is shown in Fig. 6b.

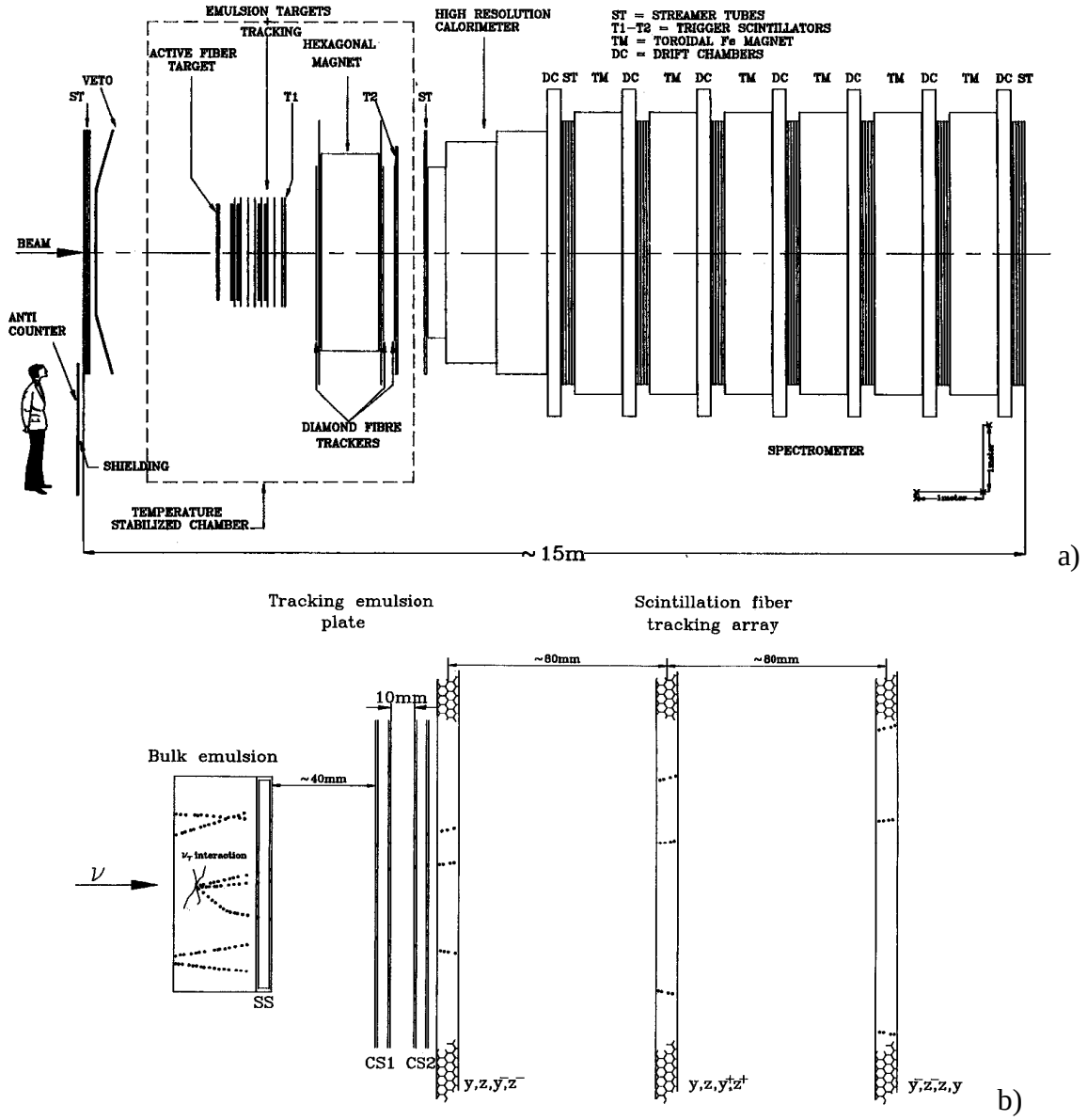

Figure 6: a) the CHORUS detector, b) a detail of the emulsion and fiber tracker in the CHORUS detector.

A bulk emulsion stack which remains in place for the duration of the experiment is followed by sheets which are changed more often and will therefore have less occupancy and by scintillations fiber trackers. The emulsions are followed by a hexagonal magnet giving a toroidal field that is constant with radius. The momentum resolution of this spectrometer is 16% at 2 GeV/*c* rising to 23% at 10 GeV/*c*. It is limited by the fact that the windings of the magnet are in the path of the particles resulting in a significant amount of multiple scattering.

The spectrometer is followed by an electromagnetic calorimeter and by a muon detector. The number of events to be scanned is reduced by a factor of 10 by applying loose kinematics cuts of the type used by NOMAD. In the surviving events tracks reconstructed in the spectrometer are extrapolated to the emulsions in order to determine where to scan. These tracks are followed into the emulsions

- to find a vertex
- to look for tracks with a kink with a p_T relative to the candidate τ direction of a least 0.24 GeV/*c*. The magnitude of this kink p_T is determined using the momentum of the

track as determined by the spectrometer and the angle of the kink as determined by the tracking in the emulsion.

The major background to the muonic channel comes from the semileptonic decays of negative charmed particles produced by the $\bar{\nu}_\mu$ and $\bar{\nu}_e$ components of the beam coupled with missing the accompanying μ^+ or e^+

$$\bar{\nu}_\mu\,(\bar{\nu}_e) + N \rightarrow X + D^- + \mu^+\,(e^+)$$
$$\qquad\qquad\qquad\qquad\quad \hookrightarrow \mu^-\ \nu_X \ \text{miss}$$

The finite travel of the D^- before its decay can thus simulate a τ decay.

In the $\tau^- \rightarrow \pi^- \nu_\tau$ channel, the major source of background is due to negative hadrons from a neutral current interaction scattering within 3 mm of the vertex without any other visible recoil activity. These so called white star kinks are very much reduced by requiring a kink p_T of at least 0.24 GeV/*c*. Further background reduction can be obtained by comparing the direction of the resultant hadronic momentum vector as calculated using the spectrometer with the direction of the τ candidate track as measured in the emulsions before the kink. For genuine τ decays these two vectors must be back to back in the plane transverse to the beam. In the background events arising from charm the μ^+ or e^+ must have been missed giving rise to missing p_T and in the white star kink events in neutral current events it is the neutrino that results in missing p_T. This missing p_T in background events causes the two vectors not to be back to back.

2.3 *E803*

This experiment [14] has been approved to run at Fermilab when the new main injector will be available. The principle of the detector, Fig. 7, is very similar to that of CHORUS. Emulsion stacks comprising both fixed bulk emulsions and changeable sheets are followed by fiber trackers, a magnet, drift chambers, an electromagnetic calorimeter and a muon detector. Since the principle of E803 is so similar to CHORUS but the experiment will run several years later, the question can be asked as to why approve E803? The answer is given in Table 2. The high repetition rate of the main injector allows E803 to expect 1.3×10^{21} protons on target as opposed to 2.4×10^{19} for CHORUS.

This in turn permits E803 to have a reduced mass target (520 kg and 2 radiation length thick). The other advantage of E803 is its better momentum resolution of 3% due to the fact that the magnet windings are not in the acceptance of the particles. The background in E803 is similar to that described for CHORUS. However, the better momentum resolution of E803 should allow a better discrimination against this background. In particular for the $\tau^- \rightarrow \pi^- \nu_\tau$ mode, a plot of the kink p_T relative to the τ direction should display the characteristic Jacobian peak at $m_\tau/2$ (Fig. 8). The collaboration has exposed emulsions to a 4 GeV/*c* pion beam at KEK. From this exposure it has been determined that white star kinks can be eliminated as a source of background with a cut of 0.3 GeV/*c* in the kink p_T. This cut also eliminates kinks from the decay of strange particles (Fig. 9).

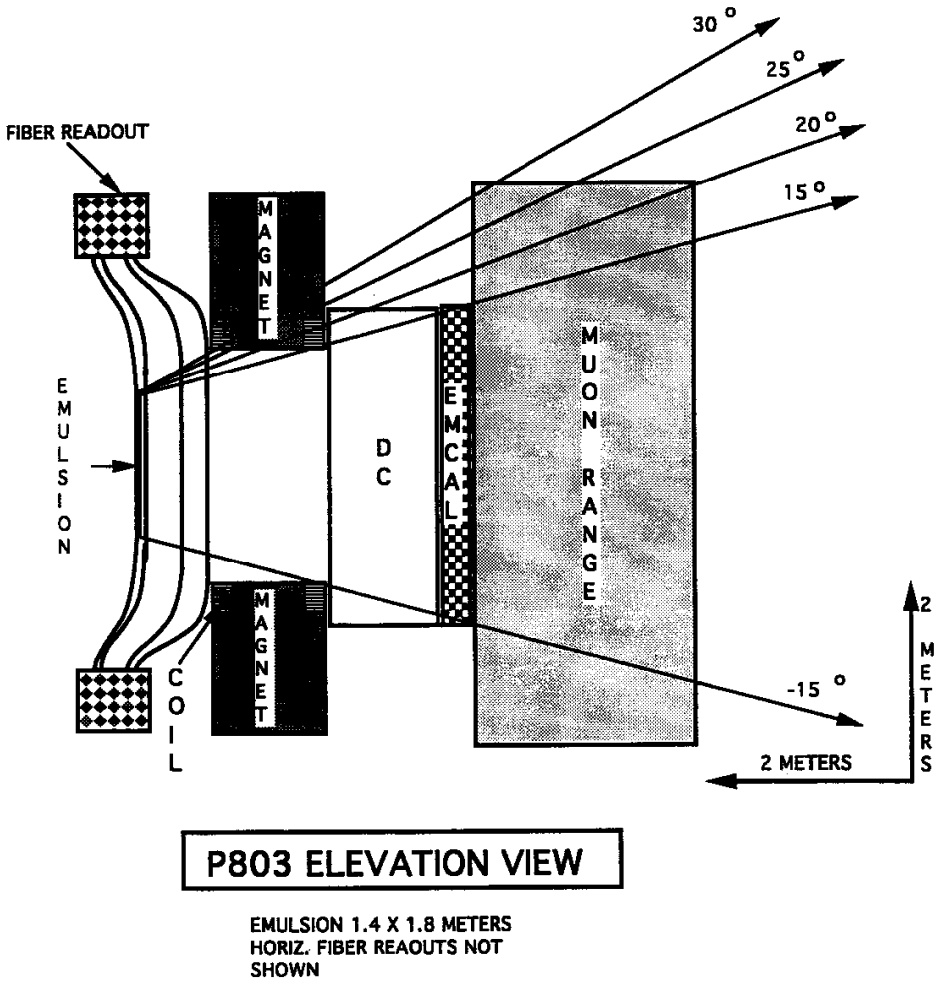

Figure 7: The E803 detector.

Table 2
Differences between CHORUS and E803

	CHORUS	E803
Protons on target	2.4×10^{19}	130×10^{19}
$\langle E_\nu \rangle$ (GeV)	27	16
Mass of target (kg)	800	520
Number of CC int.	5×10^5	60×10^5
Years	2	4
Radiation length of tgt.	4	2
Magnet	Windings in accep.	No windings
$\Delta p/p$	~ 18%	3%

The background, efficiencies and sensitivities of the three $\nu_\mu \rightarrow \nu_\tau$ oscillation experiment, CHORUS, NOMAD and E803, are listed in Table 3. It can be seen that all three experiments are sensitive to several decay modes of the τ so that if some events are observed they have to be distributed among the decay modes according to the branching ratios and efficiencies. If oscillations occurred at the limit set by E531, the CERN experiments would expect about 70 events each and E803 600 events. If no events are observed then the CERN experiments would set a limit of about 3×10^{-4} on $\sin^2 \theta_{\mu\tau}$ whereas E803, a few years later, could improve this

limit to 2.8×10^{-5}. The exclusion plot for these experiments is shown in Fig. 10. The current limits set by E531 (Ref. [2]) and CHARM II (Ref. [19]) and a limit that could be set by a liquid argon ICARUS detector [20] in the Gran Sasso fed by a ν beam from CERN are also shown.

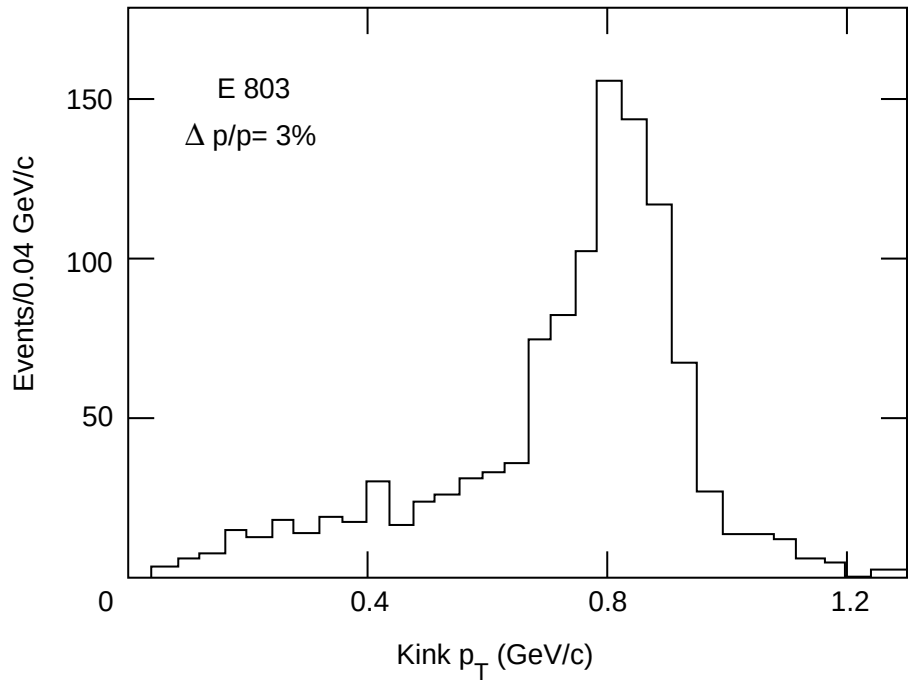

Figure 8: The $p_{T\ kink}$ distribution in $\tau^- \rightarrow \pi^- \nu_\tau$ decay showing the characteristic Jacobian peak at $m_\tau/2$.

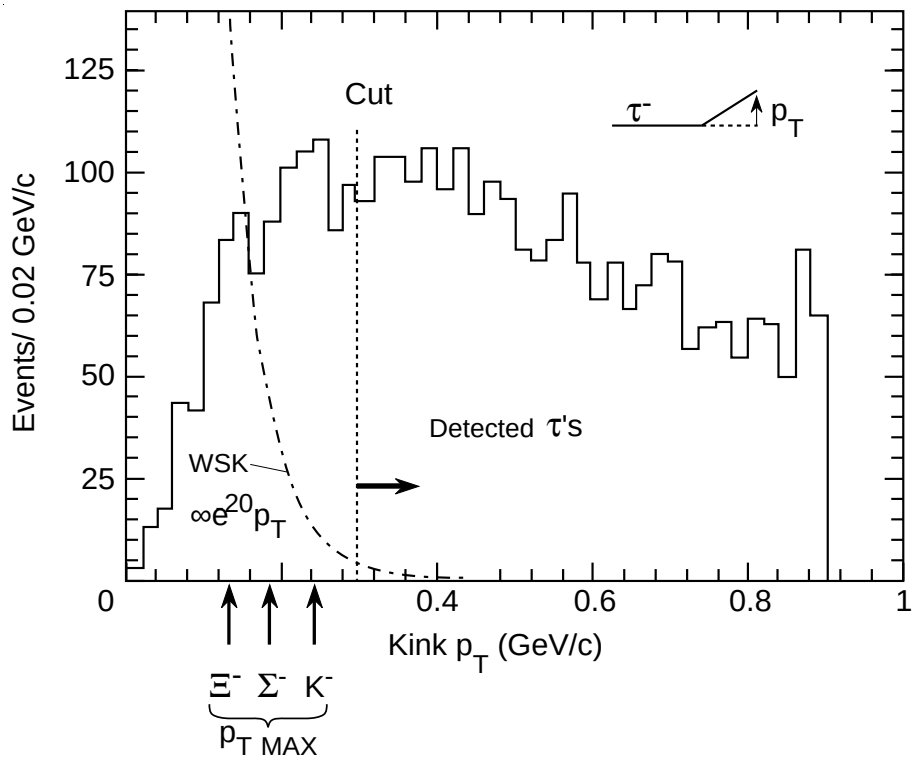

Figure 9: The $p_{T\ kink}$ distribution for all τ decays. The distribution form white star kink events is also shown as well as the maximum p_T from Ξ^-, Σ^- and K^- decay.

Table 3
Summary of background, efficiency and sensitivity for NOMAD, CHORUS, E803

	NOMAD	CHORUS	E803
Number of CC interactions	1.1×10^6	5×10^5	6×10^6
Expected running time (yrs)	≥ 2	2	4
τ decay mode	e, μ	μ	e
	$\pi^- + (n\pi^0)$	$\pi^- + (n\pi^0)$	$\pi^- + (n\pi^0)$
	$\pi^+\pi^-\pi^- +$	$\pi^+\pi^-\pi^- +$	–
Total efficiency = Σ (EFF*BR)	$(n\pi^0)$	$(n\pi^0)$	0.21
Expected number of events at the	0.048	0.096	600
E531 limit:	78	64	
Large Δm^2, $\sin^2 2\theta = 5 \times 10^{-3}$			
Expected number of background			1.2
events	6.8	0.4	
Sensitivity at large Δm^2			
$\sin^2 2\theta_{\mu\tau} <$			2.8×10^{-5}
$\sin^2 2\theta_{e\tau} <$	3.8×10^{-4}	2.8×10^{-4}	1.4×10^{-3}
Start-up date	2.7×10^{-2}	1.6×10^{-2}	1998
	1994/5	1994	

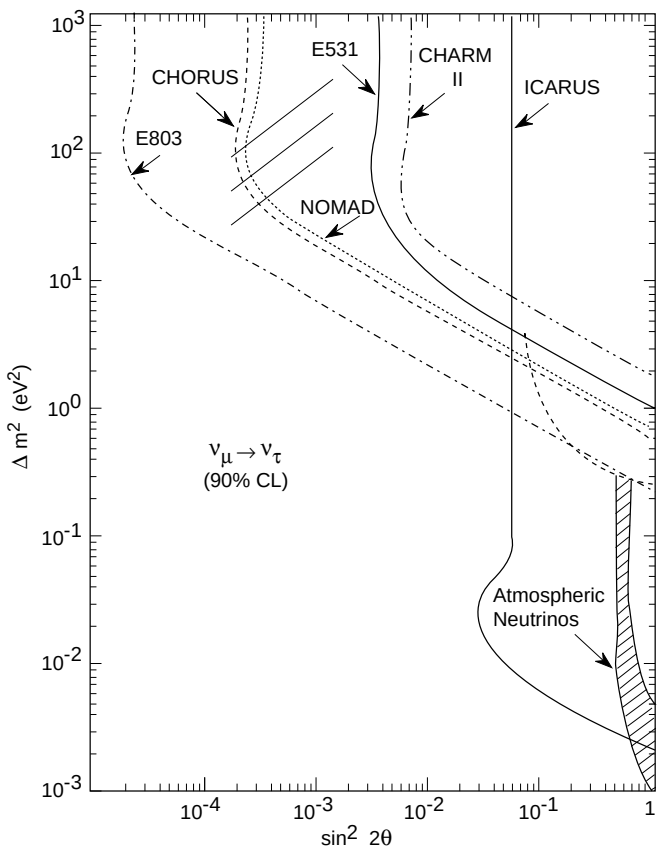

Figure 10: The regions expected to be excluded, at the 90% CL, in the Δm^2–$\sin^2 2\theta$ plot by CHORUS, NOMAD and E803 if no ν_μ–ν_τ oscillations are observed.

2.4 *Long Baseline ν Oscillation Experiment E889*

The aim of this experiment [13] is to check the atmospheric neutrino results of Kamiokande [9] and IMB [21]. The low ν_μ/ν_e ratio observed by these experiments would, if due to neutrino oscillations, imply a Δm^2 of $0.01 \rightarrow 0.1$ eV^2 and a $\sin^2\theta \sim 0.5$. The experiment intends to use a ν_μ beam with a 1% admixture of ν_e's produced by the Brookhaven AGS. It would use 3 detectors at 1,3 and 24 km from the ν source. Each detector consists of a tank of water viewed by photomultipliers. The principle of the experiment is to look for the disappearance of ν_μ's by comparing the normalised rate of $\nu_\mu\, n \rightarrow \mu\, p$ in the 3 detectors. At the same time the experiment can also look for the appearance of ν_e's though the reaction $\nu_e\, n \rightarrow e^-\, p$.

A signal for oscillations would consist of a difference in the normalised rate of ν_μ interactions in the three detectors. It is therefore very important to know the neutrino flux at the three locations. This is done by

- checking and adjusting the beam programs using the ratio of rates in the 1 and 3 km detectors. The ratio of rates in the 1 and 24 km detectors or in the 3 and 24 km detectors could then be used for the search for oscillations.
- measuring the rate of $\nu\, N \rightarrow \nu\, N'\, \pi^0$ in the 3 detectors. This neutral current reaction will occur independently of neutrino flavour and therefore independently of oscillations.

In order to separate ν_μ interactions from ν_e interactions the detector must be able to distinguish muons from electrons. This is done by the shape of the Cherenkov ring as observed by the photomultipliers.

A contained muon emits Cherenkov light along its well defined track and will therefore produce a sharp ring. A contained electron produces a shower and the angular extent of the shower results in a wider and more diffuse ring. Finally a straight through muon will emit Cherenkov light right up until it crosses the photomultiplier array resulting in a filled ring or disk.

If ν_μ's are found to disappear can they tell what they have oscillated to? As an example, Table 4 gives, for a 4 month run, event rates in the 24 km detector for $\nu_\mu n \rightarrow \mu^-\, p$, $\nu_e\, n \rightarrow e^-\, p$ and $\nu\, N \rightarrow \nu\, N'\, \pi^0$ for no oscillations and for a 6.6% loss of ν_μ due to an oscillation with parameters $\Delta m^2 = 0.01$ eV^2 and $\sin^2 2\theta = 0.5$. Three types of oscillations are considered $\nu_\mu \rightarrow \nu_e$, $\nu_\mu \rightarrow \nu_\tau$ and $\nu_\mu \rightarrow \nu_s$ (a sterile neutrino).

In the case of $\nu_\mu \rightarrow \nu_e$ oscillations, not only is a decrease in ν_μ observed, but a very large increase in ν_e interactions is observed simultaneously since the intrinsic ν_e component of the beam is only 1%. For $\nu_\mu \rightarrow \nu_\tau$ oscillations the decrease in ν_μ rate is not accompanied by a corresponding increase in ν_e rate. For both these types of oscillations the neutral current rate ($\nu N \rightarrow \nu\, N'\, \pi^0$) remains the same as for no oscillations.

Finally in the case of oscillations into a sterile neutrino the drop in ν_μ rate is accompanied by a corresponding drop in the neutral current rate.

The limit that E889 hopes to set is shown in Fig. 11. The excluded areas that have been established by CDHS [22], CHARM [23] and CCFR [24] in ν_μ disappearance experiments, and by E531 in a $\nu_\mu \rightarrow \nu_\tau$ experiment [2], by Frejus [25], and IMB [21] in atmospheric

neutrinos are also shown on the figure. The Kamiokande [9] allowed region is shown as the hatched area.

Table 4

Number of events in the 24 km detector of E889 without oscillations and with three different types of oscillations

	$\nu_\mu n \to \mu^- p$	$\nu_e n \to e^- p$	$\nu N \to \nu N' \pi^0$
No oscillation	4375	74 (1% ν_e in beam)	1108
Oscillation $\Delta m^2 = 0.01$ eV^2 $\sin^2 2\theta = 0.5$	–6.6% ν_μ's		
$\nu_\mu \leftrightarrow \nu_e$ (find the missing ν_μ's in ν_e channel)	4086	364	1108
$\nu_\mu \leftrightarrow \nu_\tau$ (find them nowhere)	4086	74	1108
$\nu_\mu \leftrightarrow \nu_{sterile}$ (find them nowhere and NC's drop since ν_s cannot contribute)	4086	74	1035

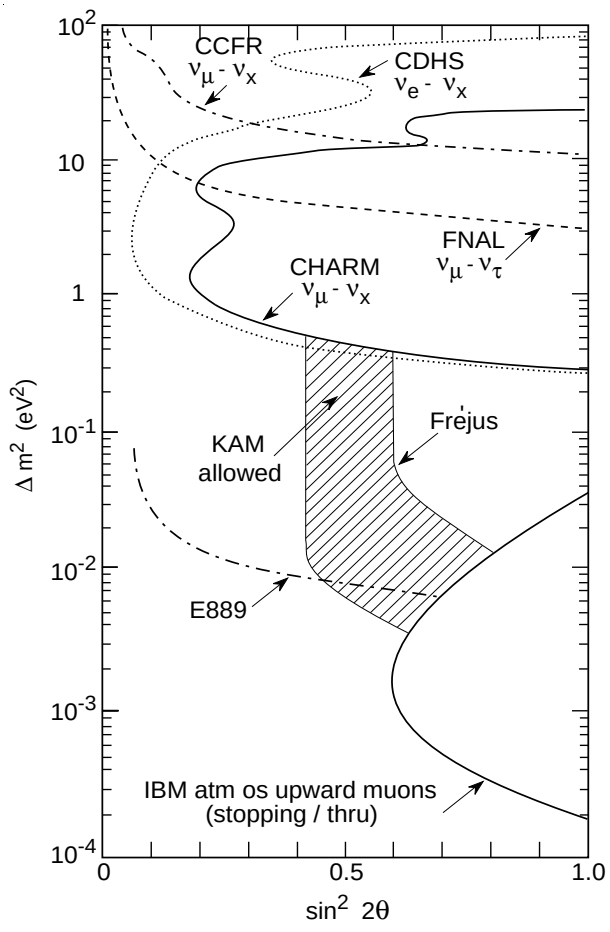

Figure 11: The region expected to be excluded by E889 in the Δm^2–$\sin^2 2\theta$ by E889 if no ν_μ–ν_x oscillations are observed.

3 Conclusions

There are 5 experiments which are running, about to run or about to be built. They will improve the limits on $\nu_\mu \to \nu_e$, $\nu_\mu \to \nu_x$ and $\nu_\mu \to \nu_\tau$, thereby

- checking the atmospheric neutrino results
- probing $\nu_\mu \to \nu_\tau$ oscillations in a Δm^2 and $\sin^2 2\theta$ region which is favoured by solar neutrino and the see-saw mechanism and by hot dark matter.

References

[1] B. Pontecorvo, *Zh. Eksp. Theor. Fiz.* **33** (1957) 549 and **34** (1958) 247.

[2] N. Ushida et al., *Phys. Rev. Lett.* **57** (1986) 2897.

[3] J. Ellis et al., CERN–TH 6569/92 (1992) and the contributions by G. Altarelli and J. Ellis in these proceedings.

[4] For the latest results on solar neutrinos see the contributions by the R. Davis, Y. Suzuki, V.N. Gavrin and C. Cattadori in these proceedings.

[5] L. Wolfenstein, *Phys. Rev.* **D17** (1978) 2369;
S.P. Mikheyev and A.Y. Smirnov, *Sov. J. Nucl. Phys.* **42** (1985) 913.

[6] M. Gell-Mann, P. Ramond and R. Slansky *in* Supergravity, ed. P. van Nieuwenhuizen and D. Freedman (North Holland, Amsterdam, 1979), p. 315.

[7] T. Yanagida, *Prog. Theor. Phys.* **B135** (1978) 66.

[8] S.F. Shandarin, Massive Neutrinos and Cosmology *in* Neutrino Physics, edited by Klaus Winter (Cambridge Monographs on Particle Physics, Nuclear Physics and Cosmology,) p. 645 and references therein.

[9] K.S. Hirata et al., *Phys. Lett.* **280B** (1992) 146 and Kamiokande contribution to this conference (Y. Suzuki).

[10] Liquid Scintillator Neutrino Detector (LSND).
A proposal to search for Neutrino Oscillations with High Sensitivity in the Appearance channels $\nu_\mu \to \nu_e$ and $\bar{\nu}_\mu \to \bar{\nu}_e$. Proposal to Los Alamos Meson Physics facility (1989).

[11] CERN Hybrid Oscillation Research Apparatus (CHORUS). A new search for $\nu_\mu \to \nu_\tau$ oscillation, CERN–PPE/93–131 (1993) and CERN–SPSC/90–42 SPSC P254.

[12] Neutrino Oscillation Magnetic Detector (NOMAD). Search for the Oscillation $\nu_\mu \to \nu_\tau$, CERN–SPSLC/91–21 SPSC P261 (1991) and CERN–SPSLC/93–31 SPSLC M525 (1993).

[13] Proposal for a Long Baseline Neutrino Oscillation Experiment at the AGS E–889 (1993).

[14] Muon Neutrino to Tau Neutrino Oscillations Experiment E803 at Fermilab.

[15] V. Zacek et al., *Phys. Lett.* **164B** (1985) 193.

[16] L.A. Ahrens et al., *Phys. Rev.* **D31** (1985) 2732.

[17] L.S. Durkin et al., *Phys. Rev. Lett.* **61** (1988) 1811;
James J. Napolitano et al., *Nucl. Instrum. Methods Phys. Res.* **A274** (1989) 152.

[18] T. Dombeck et al., *Phys. Lett.* **B194** (1987) 591.

[19] M. Gruwé et al., Phys. Lett. B309 (1993) 463.

[20] ICARUS II A Second Generation Proton Decay Experiment and Neutrino Observatory at the Gran Sasso Laboratory. Proposal by the ICARUS Collaboration (1993).

[21] D. Casper et al., *Phys. Rev. Lett.* **66** (1991) 2561 and IMB contribution to this conference.

[22] F. Dydak et al., *Phys. Lett.* **134B** (1984) 281.

[23] F. Bergsma et al., *Phys. Lett.* **142B** (1984) 103.

[24] C. Haber et al., Fermilab Preprint Fermilab Conf. 83/57 Exp. (1983).

[25] Ch. Berger et al., *Phys. Lett.* **B245** (1990) 305.